Stochastic Modelling and Computational Sciences

ANALYSIS OF HEAT TRANSFER IN TERNARY HYBRID NANOFLUIDS OVER A STRETCHING SHEET WITH RADIATION AND HEAT SOURCE USING MACHINE LEARNING ALGORITHM

A. Haritha[1,*], Y. Devasena[2] and D. Rohith Rayal[3]
[1,2]Assistant Professor, Department of BS&H, SoET, Sri Padmavati Mahila Visvavidyalayam, Tirupati, A.P, India
[3]II B.Tech, C.S.E (AI&ML), Mohan Babu University, Tirupati, A.P, India

ABSTRACT
The present paper includes the study of heat transfer of ternary hybrid nanofluid flow over a stretching sheet influenced by thermal radiation, magnetic field and heat source with convective boundary conditions. In this model Cu, Fe_3O_4 and SiO_2 are treated as nanoparticles suspended in the base fluid H_2O to form the tri hybrid nanofluid. The governing partial differential equations pertaining to the mathematical model describing the physics of the study aretransformed to ordinary differential equations and resolved numerically by employing Runge-Kutta fourth order method with shooting scheme. The plots of velocity and temperature profiles for both $Cu+Fe_3O_4+SiO_2/H_2O$ and $Cu+SiO_2/H_2O$ for various parameters are captured and deliberated using MATLAB solver bvp4c. Further Machine learning tools are applied to forecast rate of heat transfer and frictional drag by captivating hyperplane using SVM algorithm also MSE, RMSE, MAE, MAPE and R^2 are evaluated to assess the error between true and predicted values. In the realm of friction rate assessment, a higher R^2 value serves as a marker for the efficiency of the proposed SVM model. Likewise, when dealing with variations in Nusselt number concerning both heat source and radiation parameter, increased MAE and R^2 error values underscore a higher level of precision in the analysis. The presented values shows that the modelling of the problem has greater accuracy and endorses that ternary nanofluid has an excellent thermal accomplishment over the hybrid nanofluid.The ongoing optimization process has uncovered novel insights that can significantly enhance the production method for plastic films, heat exchangers, polymer sheets and electronic devices. As, a result the findings obtained are highly recommended for incorporation into the development of industrial equipment setups.

Keywords: ternary hybrid nanofluid; convective boundary conditions; machine learning; support vector machine

1. INTRODUCTION
Understanding and controlling heat transfer are essential in various fields, including engineering, physics, environmental science and material science. Engineers and scientists often utilize heat transfer principles to design efficient heating and cooling sysems, optimize energy usage and improve the performance of devices and processes. There has been a considerable focus on developing smarter strategies for heat management, aiming to enhance efficiency without expanding the physical footprint of cooling systems. One such area of focus is the utilization of nanofluids, a novel class of heat transfer fluids, have garnered significant attention due to their promising potential for enhancing heat transfer performance in various applications. These nanofluids consist of base fluids (such as water, ethylene glycol, or oil) that are infused with nanoparticles, typically metallic or non-metallic in nature, with sizes ranging from 1 to 100 nanometers. The presence of nanoparticles in nanofluids alters their thermal properties, leading to improved heat transfer characteristics compared to traditional heat transfer fluids. The unique characteristics of nanoparticles, such as their high thermal conductivity and surface area-to-volume ratio, make the role of nanofluids in advancing thermal management technologies. [1] Choi and eastman in 1995 proposed an intriguing idea of adding nanoparticles to fluids which enhances the heat transfer capabilities of base liquids. Chiam et al. [2] observed a direct correlation between the volume concentration of nanoparticles and the resulting enhancement in thermal conductivity. Small alterations in thermophysical properties can lead to considerable changes in the material characteristics of nanofluids, these leads to analze the nanofluid material properties as given in [3-6].

Subsequent investigations revealed that dipersing multiple nanosized particles within a transparent fluid can enhance the thermal proprties of the base fluid which are termed as hybrid nanofluids. Hybrid nanofluids have emerged as efficient solutions for dissipating heat in thermal systems operating at elevated temperatures. These

advanced fluids find extensive thermal applications, particularly in solar energy systems, heat exchangers, cooling mechanisms for generators and transformers, as well as nuclear power plants. Huang et al.[7] demonstrated the attributes of mixture of hybrid nanofluid over heated plate exchanger showing that the mixture has maximum heat transfer coefficient. Emad and Pop [8] investigated the heat transfer in the MHD flow of hybrid nanofluids over a convectively heated stretching sheet.For stretching sheet it was shown that adding nanoparticles of Cu-Al_2O_3/H_2O cools the resulting hybrid nanofluid by increasing magnetic field and mass flux parameters when compared to nanofluids. Cu-Al_2O_3/H_2O hybrid nanofluid flow past a porous stretching sheet due to temperature dependent viscosity and viscous dissipation was studied by Satya Narayana et al. [9]. The results indicated that the velocity profile for hybrid nanofluid increases with increase of convection parameter and due to presence of variable viscosity the hybrid nanofluid converges to the boundary more fast than that of the Al_2O_3/H_2O nanofluid. Many research studies on hybrid nanoparticle mixture, applications and its development are given in references[10-12] , it is observed that the hybrid nanofluids have superior heat transfer performance and thermophysical properties when compared with single nanofluid.

Recently, researchers have introduced an innovative approach by blending three distinct types of nanoparticles into a pure fluid, paving the way for a new class called Ternary hybrid nanofluids,which have better thermal conductivity and dynamic viscosity than mono and hybrid nanofluids. This is due to the unique properties of the individual nanoparticles in the ternary mixture. Jafar Hasnain et al.[13] studied thermal growth in water and engine oil-based ternary nanofluid using three different shaped nanoparticles over a linear and nonlinear stretching sheet, it concludes that when volume fraction of nanoparticle increases temperature increases in the case of ternary nanofluid over a linearly stretching sheet and nonlinearly stretching sheet as compared to hybrid nanofluid. Theoretical study of convective heat transfer in Ternary nanofluid flowing past a stretching sheet was studied by anjunatha et al.[14] and observed that tri hybrid nanofluid shows better thermal conductivity than that of hybrid nanofluid. The ternary hybrid nanofluid ($CuO+TiO_2+MgO/H_2O$) behaviour was analyzed by Mosavi et al.[15]. Adnan and Ashraf [16] explicated the effect of a magnetic field with convective heating on a Trihybrid nanofluid flow and exhibited a comparison of THNF and hybrid nanofluid flow. Recent studies focusing on trihybrid nanofluids have sparked additional intrest and prompted further investigation [17-20].

The interaction of multiple nanoparticle species within the fluid matrix introduces complexities that traditional analytical methods struggle to address comprehensively. Therefore, the utilization of machine learning algorithms presents a novel approach to model and understand the intricate heat transfer dynamics in such complex systems. Machine learning algorithms have shown great potential in various scientific and engineering disciplines for their ability to analyze large datasets and extract meaningful patterns and insights. Among various machine learning algorithms, support vector machine (svm) models are versatile that can be applied to a wide range of problems across various domains. Svms have been applied in various sectors as it handle tasks where the data is not linearly separable by using kernel functions. Svms perform well in high-dimensional spaces, making them suitable for problems with many features or variables, this property is particularly valuable in fields like genomics, bioinformatics, medical diagnosis and image processing, where datasets often have a large number of dimensions. Perspective on machine learning for advancing fluid mechanics was investigated by brenner et al.[21]. Rehman et al. [22] predicted skin friction values using ann model in non-newtonian mixed convection magnetized flow with heat generation and viscous dissipation effects: a prediction application of artificial intelligence and found that sfc values are high in magnitude in an inclined cylindrical surface to that of flat surface. Priyadarshini et al. [23] presented a gradient descent regression technique to forecast the physical features for mhd flow. Recently some investigations on nanofluids with machine learning technique have attracted for further study [24-26] .

This study focuses on employing SVM algorithm to analyze heat transfer characteristics in ($Cu+Fe_3O_4+SiO_2/H_2O$) ternary hybrid nanofluids over a stretching sheet, accounting for Magnetic field (M), radiation effect (R) and the presence of a heat source (Q). The review was carried out in two different ways, first approach is that partial differential equations are solved numerically by employing Runge-Kutta fourth order method with shooting scheme then second by employing Support Vector Machine (SVM) model a machine learning technique to

examine Sherwood number and Nusselt number with respect to M, R and Q. The radar plot utilized in the research served the purpose of comparing actual and predicted values through various evaluation metrics, the higher R^2, MAE values of friction rate and Nusselt number denotes effectiveness of SVM model.

2. MATHEMATICAL FORMULATION:

We analyse the steady two-dimensional MHD boundary layer flow of a ternary hybrid nanofluid over a convectively heated elastic sheet. The ternary hybrid nanofluid is the blend of Cu nanoparticles, iron oxide(Fe_3O_4) and aluminium-oxide particles (Al_2O_3) with water as host fluid. The physical geometry of the flow model is outlined in Fig.(1). The x-axis is chosen in the direction of the flow and y-axis is normal to it. The horizontal velocity is as $U_w(x) = ax$ (a is constant with dimension t^{-1}), T_w is the wall temperature and $T_\infty$is the ambient temperature. A uniform transverse magnetic field of strength B_0 is applied perpendicular to X-axis. Applying the thermal radiation with conventional boundary conditions the governing equations of ternary hybrid nanofluid flow are as follows [14],

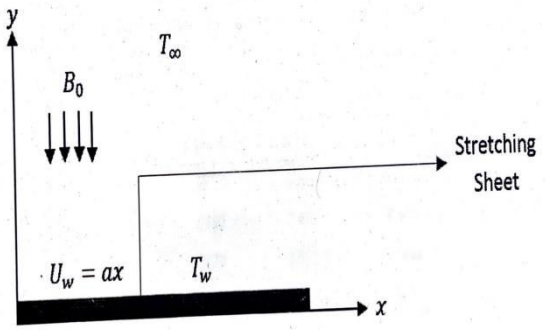

Fig. (1) Geometry of the flow configuration

$$\frac{\partial u}{\partial x} + \frac{\partial v}{\partial y} = 0, \quad (1)$$

$$u\frac{\partial u}{\partial x} + v\frac{\partial u}{\partial y} = \frac{\mu_{thnf}}{\rho_{thnf}}\frac{\partial^2 u}{\partial y^2} - \frac{\sigma_{thnf}}{\rho_{thnf}}B_0{}^2 u \quad (2)$$

$$(\rho C_p)_{thnf}\left\{u\frac{\partial T}{\partial x} + v\frac{\partial T}{\partial y}\right\} = k_{thnf}\frac{\partial^2 T}{\partial y^2} - \frac{\partial q_r}{\partial y} + Q(T - T_\infty) \quad (3)$$

The suitable boundary constraints are:

$$u = u_w,\ v = 0,\ -k_{thnf}\frac{\partial T}{\partial y} = h_f(T_w - T) \text{ at } y = 0, \quad (4)$$

$$u \to 0, \quad T \to T_\infty \quad as \quad y \to \infty.$$

The scaling analysis is given hereunder:

$$\eta = \sqrt{\frac{a}{\nu_f}}y,\ \theta(\eta) = \frac{T - T_\infty}{T_w - T_0},\ u = axf'(\eta), v = -(\nu_f a)^{1/2} f(\eta) \quad (5)$$

The radiative heat flux $q_r$using Roseland approximation [27] is defined as follows

$$q_r = \frac{-4\sigma^*}{3k^*}\frac{\partial T^4}{\partial y} \quad (6)$$

Using Taylor's series the expansion of T^4 about T_∞ is given as

$$T^4 \approx 4T_\infty^3 T - 3T_\infty^4 \quad (7)$$

Using equations (6) and (7), equation (3) reduces to the following form

$$u\frac{\partial T}{\partial x} + v\frac{\partial T}{\partial y} = \frac{k_{thnf}}{(\rho C_p)_{thnf}}\frac{\partial^2 T}{\partial y^2} + \frac{16\sigma^* T_\infty^3}{3k^*(\rho C_p)_{thnf}}\frac{\partial^2 T}{\partial y^2} + \frac{1}{(\rho C_p)_{thnf}}Q(T - T_\infty) \quad (8)$$

Substituting equations (4), (5) the governing equations (2) and (8), reduce to

$$\frac{\mu_{thnf}}{\mu_f}f''' + \frac{\rho_{thnf}}{\rho_f}(ff'' - f'^2) - \frac{\sigma_{thnf}}{\sigma_f}Mf' = 0 \quad (9)$$

$$\frac{1}{Pr}\left(\frac{k_{thnf}}{k_f} + \frac{4}{3}R\right)\theta'' + \frac{(\rho C_p)_{thnf}}{(\rho C_p)_f}f\theta' + Q\theta = 0. \quad (10)$$

The associated constraints on the boundary:

$$f(0) = 0, f'(0) = 0, f' \to 0 \ \ as \ \ \eta \to \infty \ , \quad (11)$$

$$\theta'(0) = -Bi\frac{k_{thnf}}{k_f}\{1 - \theta(0)\},' \ \ \theta \to 0 \ as \ \eta \to \infty$$

Where M = $\frac{\sigma B_0^2}{a\rho_f}$ is the Magnetic field parameter, Pr = $\frac{\vartheta_f(\rho c_p)_f}{k_f}$ is Prandtl number, R= $\frac{4\sigma^* T_\infty^3}{k^* k_f}$ is radiation parameter,

Q = $\frac{Q^*}{a(\rho C_p)_f}$ is heat source parameter and Bi = $\frac{h_f}{k_f}\sqrt{\frac{\vartheta_f}{a}}$ is Biot number.

C_f (Frictional coefficient), Nu_x(Nusselt number) at the boundary are defined by

$$C_f = \frac{\tau_w}{\rho_f u_w^2} \ \ and \ \ Nu_x = \frac{x q_w}{k_f(T_w - T_0)} \quad (12)$$

where, $\tau_w = \mu_{thnf}\left(\frac{\partial u}{\partial y}\right)_{y=0}$, $q_w = -k_{thnf}\left(1 + \frac{16\sigma^* T^3}{3k_{hnf}k^*}\right)\left(\frac{\partial T}{\partial y}\right)_{y=0}$

Making use of Eq. (5), Eq. (12) reduces to

$$C_f\sqrt{Re_x} = \frac{\mu_{thnf}}{\mu_f}f''(0), \ \ Nu_x/\sqrt{Re_x} = -\frac{k_{thnf}}{k_f}\theta'(0). \quad (13)$$

Thermophysical characteristics of the nanoparticles and base fluid [14, 28] are detailed in Table 1.

Table 1: Nanoparticles values

Nanofluid Particles				**Base fluid**
Thermophysical properties	Cu	Fe_3O_4	SiO_2	H_2O
Thermal conductivity (K_f), W/m.k	400	9.7	1.4013	0.6071
Heat capacity (C_p), J/k	385	670	765	4179
Density(ρ), kg/m^3	8933	5180	2270	997.1
$\sigma(s/m)$	5.96×10^7	2.5×10^{-4}	3.5×10^6	5.5×10^{-6}

Table 2: Nanoparticle properties

Thermophysical properties	Ternary Hybrid Nanofluid
Thermal conductivity (K_f), W/m.k	$\frac{k_{nf}}{k_f} = \frac{k_s+2k_f-2\phi_s(k_f-k_s)}{k_s+2k_f+\phi_s(k_f-k_s)}$, $\frac{k_{hnf}}{k_{nf}} = \frac{k_2+2k_{nf}-2\phi_2(k_{nf}-k_2)}{k_2+2k_{nf}+\phi_2(k_{nf}-k_2)}$, $\frac{k_{thnf}}{k_{hnf}} = \frac{k_1+2k_{hnf}-2\phi_1(k_{hnf}-k_1)}{k_1+2k_{hnf}+\phi_1(k_{hnf}-k_1)}$
Heat capacity (C_p), J/k	$(\rho C_p)_{thnf} = (1-\phi_1)[(1-\phi_2)[(1-\phi_3)+\phi_3\frac{(\rho C_p)_3}{(\rho C_p)_f}]+\phi_2\frac{(\rho C_p)_2}{(\rho C_p)_f}]+\phi_1\frac{(\rho C_p)_1}{(\rho C_p)_f}$
Density(ρ), kg/m^3	$(\rho)_{thnf} = (1-\phi_1)[(1-\phi_2)[(1-\phi_3)+\phi_3\frac{\rho_3}{\rho_f}]+\phi_2\frac{\rho_2}{\rho_f}]+\phi_1\frac{\rho_1}{\rho_f}$
Viscosity (μ), N.s/m^2	$\mu_{thnf} = [(1-\phi_1)]^{-2.5}[(1-\phi_2)]^{-2.5}[(1-\phi_3)]^{-2.5}\mu_f$
Electrical conductivity	$\frac{\sigma_{nf}}{\sigma_f} = \frac{\sigma_s(1+2\phi_s)+\sigma_f(1-2\phi_s)}{\sigma_s(1-\phi_s)+\sigma_f(1+\phi_s)}$, $\frac{\sigma_{hnf}}{\sigma_{nf}} = \frac{\sigma_2(1+2\phi_2)+\sigma_{nf}(1-2\phi_2)}{\sigma_2(1-\phi_2)+\sigma_{nf}(1+\phi_2)}$, $\frac{\sigma_{thnf}}{\sigma_{hnf}} = \frac{\sigma_1(1+2\phi_1)+\sigma_{hnf}(1-2\phi_1)}{\sigma_1(1-\phi_1)+\sigma_{hnf}(1+\phi_1)}$

Table 3: Comparison of the present results withManjunatha et al [14] cocerning the rate of heat transfer and friction rate for different values of Pr when R = 0.

Pr	Manjunatha et al	Khan and Pop	Present Result
2	0.9113	0.9113	0.9114
6.13	1.7596	1.7597	1.7595
20	3.3539	3.3539	3.3538

3. Machine Learning Scheme:

In the specified region, the optimal parameters for nanofluids were determined through numerical analysis. To know deeper into their impact, an iterative methodology was employed to assess various parameters. Given the nanoparticles high sensitivity to magnetic fields, key parameters such as the magnetic parameter (M), heat source parameter (Q), and radiation parameter (R) were introduced to the fluid within defined ranges $0.5 \leq M \leq 5$, $0.1 \leq Q \leq 0.5$ and $0.1 \leq Q \leq 0.5$. The dataset was partitioned into training and testing subsets to facilitate thorough analysis.

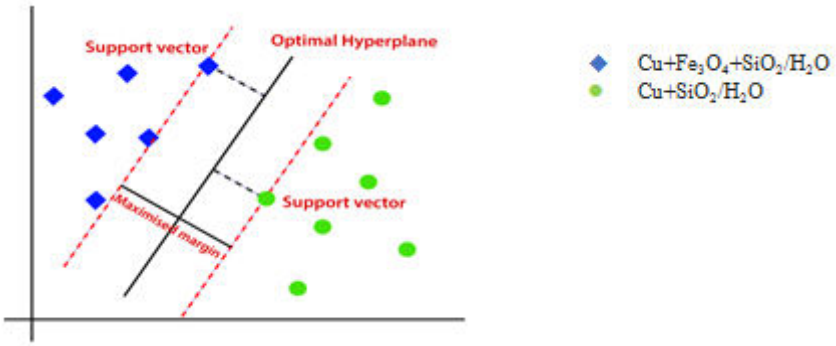

Fig. (2) Graphical representation of SVM.

Regression, a prominent machine learning approach, leverages independent variables to predict the values of target variables [29-31]. Operating within the framework of supervised learning, regression necessitates labeled data for training. Its primary objective is to establish relationships between input variables and predictions. Different regression models vary in their treatment of the correlation between independent and dependent

variables, as well as the number of independent variables considered. In this study, Support Vector Machine (SVM) emerges as a chosen prediction algorithm. SVM is a type of regression algorithm which identifies the optimal hyperplane with maximum margin from support vectors. Employing structural risk minimization, SVMs mitigate model error.The core principle of SVM setup, illustrated in Figure 2, revolves around identifying support vectors to classify data into two classes based on summarized data information. SVMs find applications across various research domains, including social sciences, engineering, and biomedicine.

Consider the regression function as

$$f(\xi) = \sum_{i=1}^{N} W_i . \varphi(\varsigma) + B \qquad (14)$$

Here $\varsigma = \varsigma_1, \varsigma_2, \ldots \varsigma_N$ are input variables such as M, R, Q, Bi and $\xi = \xi_1, \xi_2, \ldots \xi_N$ are target variables such as skin friction coefficient and nusselt nuber, $f(\xi)$ represents regression function that predicts target variable, W_i is the i^{th} element of the regression coefficient, B is the intercept term, a constant value added to the prediction. After developing the regression function, the SVM classifies the heat transfer rate and friction rate of the hybrid nanofluid and tri hybrid nanofluid into two classes. In machine learning, ensuring model accuracy through validation is crucial. This involves assessing the model's predictive capabilities using various performance metrics. In this study, five key metrics were utilized to comprehensively evaluate the forecasting models: mean square error (MSE), root mean square error (RMSE), mean absolute error (MAE), mean absolute percentage error (MAPE), and coefficient of determination (R^2).

$$\text{MSE} = \frac{1}{N}\sum_{i=1}^{N}(\xi_i - \widehat{\xi_i})^2, \quad \text{MAE} = \frac{1}{N}\sum_{i=1}^{N}\left|\xi_i - \widehat{\xi_i}\right|, \quad \text{RMSE} = \sqrt{\frac{1}{N}\sum_{i=1}^{N}(\xi_i - \widehat{\xi_i})^2}$$

$$\text{MAPE} = \frac{1}{N}\sum_{i=1}^{N}\left|\frac{\xi_i - \widehat{\xi_i}}{\xi_i}\right|, \quad R^2 = 1 - \frac{\sum_{i=1}^{N}(\xi_i - \widehat{\xi_i})^2}{\sum_{i=1}^{N}(\xi_i - \widehat{\xi_i})^2} \qquad (15)$$

4. RESULTS AND DISCUSSION:

The set of higher order nonlinear equations (9) and (10) with the suitable boundary equations (11) are numerically addressed employing MATLAB. This section aims to elicit the influence of various parameters namely M (Magnetic field Parameter), Bi (Biot number), R (Radiation), Pr (Prandtl number) and Q (Heat source parameter) on velocity, temperature, coefficient of frictional drag and heat transport in the case of $Cu+Fe_3O_4+SiO_2/H_2O$ Trihybrid nanofluid phase and $Cu+SiO_2/H_2O$ nanofluid phase and are graphically projected through Figs. (3-6). A very good agreement is found by comparing results [14, 32] when R = 0 shown in table (3)

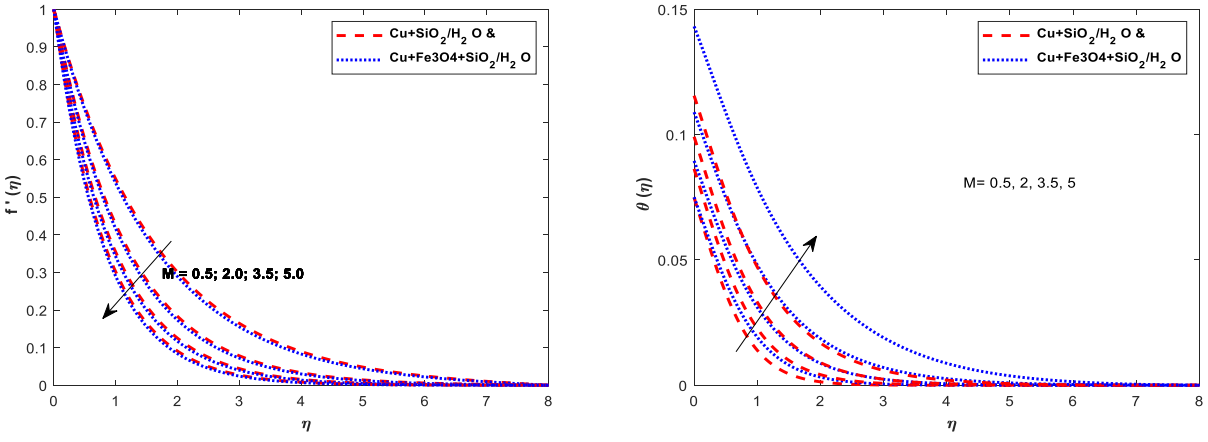

(a) **(b)**

Fig. (3) Impact of Magnetic parameter M on (a) $f'(\eta)$ and (b) $\theta(\eta)$

Fig. (3) represents the plots of velocity and temperature presenting the impact of Magnetic body force (M). It infers that the velocity of trihybrid nanofluid ($Cu+Fe_3O_4+SiO_2/H_2O$) is slightly higher than that of ($Cu+SiO_2/H_2O$) HNF. Evidently the velocity reduces with increase in the intensity of the magnetic field. This behaviour may be due to the fact that the Lorentzian force induced by the magnetic field as a retarding impact leading to the reduction in the linear momentum. The velocities are further declined due to increased resistance. The THNF shows a greater thermal measure when compared with HNF and the thermal measure for both fluids shows a hike with increasing magnetic parameter (M). Physically, the increased resistance due to Lorentz force creates more frictional heat which heats up the fluid and hence higher thermal measures prevail.

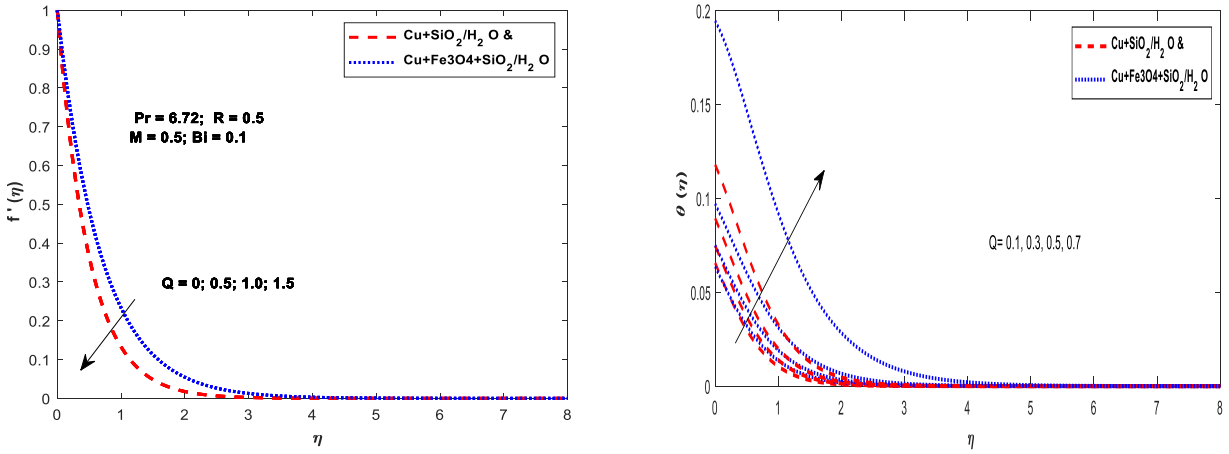

(a) **(b)**

Fig. (3) Impact of heat source parameter Q on (a) $f'(\eta)$ and (b) $\theta(\eta)$

Figs.(3) illustrates the response of velocity and heat measure to heat source parameter Q. A fall in velocity is observed with increased values of Q. However, the temperature is upsurged with higher intensities of the heat generation (Q) due to the additional supply of thermal energy to the fluid. .Further, the temperature distribution shoots up continuously through convection and thus leads to an enhancement in the temperature of the boundary layer forming thickening the thermal boundary layers. Also, it is seen that the trihybrid phase has more momentum and heat transfer when compared with hybrid phase.

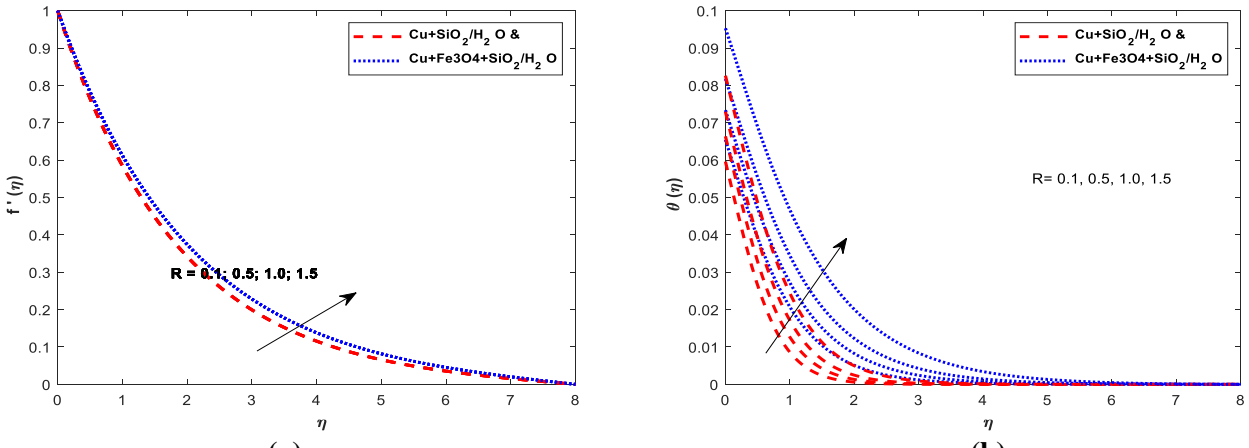

(a) **(b)**

Fig. (4) Impact of Radiation parameter R on (a)$f'(\eta)$ and (b) $\theta(\eta)$

Fig.(4) projects the influence of R on velocity and temperature in THNF and HNFcases. It is observed that R exhibits incremental enhancement both on velocity and temperature, this is as the heat flux increases fluid heats up resulting in elevated temperatures across the fluid medium.

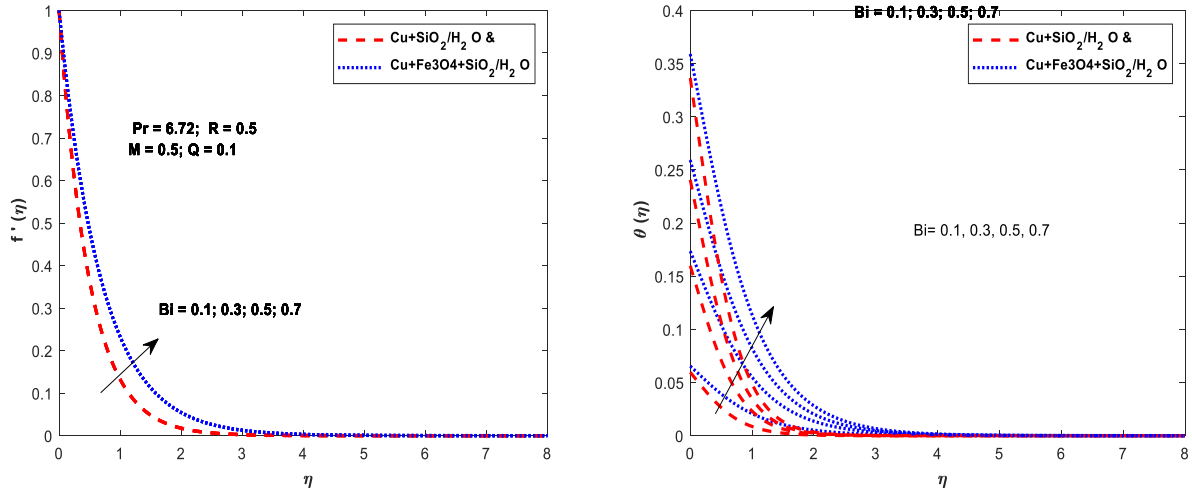

(a) (b)

Fig. (5) Influence of Biot number Bi on (a) $f'(\eta)$ and (b) $\theta(\eta)$

Fig. (5) exhibits the effect of convective heat transfer parameter Bi on velocity and temperature respectively. It shows that an increase in convective heat transfer parameter Bi=$\frac{h_f}{k_f}\sqrt{\frac{\vartheta_f}{a}}$ increases dimensionless velocity, this is due to Bi is directly proportional to heat transfer coefficient and release of thermal energy . A rise in the Biot number (Bi) leads to an augmentation in temperature, primarily due to the increased supply of heat from the hot boundary to the surrounding fluid. This heightened supply results in a swift escalation in temperature, particularly in the vicinity near the wall.

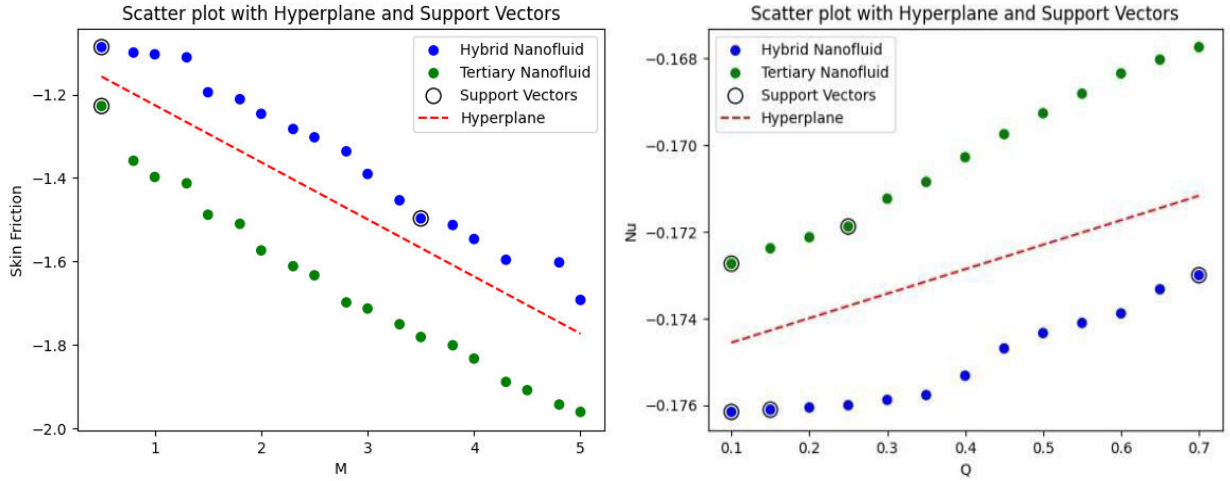

(a)99%, C= 2000 **(b)99%, C= 1,50,000**

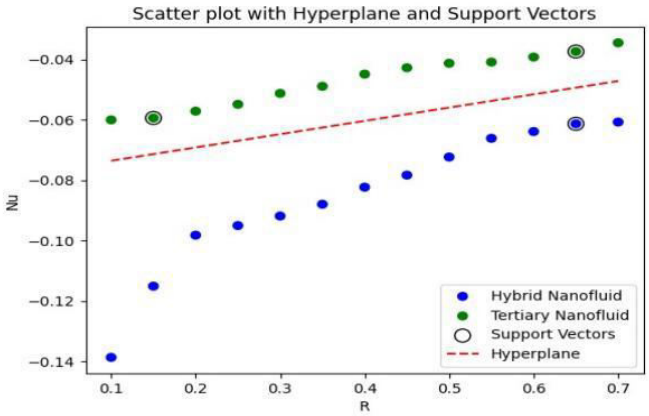

(c) 100%, C = 15,000

Fig. (6) Classification behaviour of ternary and hybrid nanofluids using SVM.

4.1 Result based on Machine Learning model:

Fig. (6) illustrates the SVM classification performance by constructing a hyperplane across 30 datasets. In Fig. 6(a), the skin friction coefficient is shown concerning the magnetic parameter ranging from 0.5 to 5. For the hybrid nanofluid, the friction rates were recorded as 1.086155 and -1.692417, while for the ternary hybrid nanofluid, they were -1.227399 and 1.960994. Notably, the support vectors for both fluids are highlighted in the figure, suggesting that increasing the magnetic parameter led to a decrease in the friction rate. Moving on to

Fig. 6(b) and 6(c), the Nusselt number is depicted concerning the variation of the heat source parameter and volume fraction within the range of 0.1 to 0.7. For the heat source parameter, the heat transfer rates for the hybrid and ternary hybrid nanofluids were -0.176155, -0.173007, and -0.172739, -0.167748 respectively. As for an increase in radiation parameter, the heat transfer rates for the hybrid nanofluid and the ternary hybrid nanofluid were -0.13871, -0.06074, and -0.06002, -0.03448 respectively. These results indicate that the heat source/sink exhibited superior heat transfer rates based on the Nusselt number analysis.

The radar plot featured in the study served to compare actual and predicted values using evaluation metrics such as Mean Squared Error (MSE), Root Mean Squared Error (RMSE), Mean Absolute Error (MAE), Mean Absolute Percentage Error (MAPE), and R^2. Fig. (7) emphasizes the computed accuracy results concerning friction rate and heat transfer rates. For friction rate assessment, a higher R^2 value denotes the effectiveness of the proposed SVM model. Similarly, elevated MAE and R^2 error values regarding Nusselt number variation with heat source and radiation parameter signify precision. This radar plot provides valuable visual insights into the distribution of data points, class separability, hyperplane orientation, and model performance along M,Q and R dimensions. These findings contribute to a comprehensive understanding of the SVM model's effectiveness in classifying ternary nanofluids and can be leveraged to inform further research and application in the field. Additionally, Table 4 lists training and testing error values, indicating the disparity between true and predicted values in terms of error. Notably, the results demonstrate strong agreement between anticipated and numerically simulated findings of the checking dataset, with minimal error.

Table (4): Training and Testing error values

Dataset	parameter	Physical quantities	MSE	RMSE	MAE	MAPE	R^2
Training Testing	M	$f''(0)$	0.0344800 0	0.1856900 0	0.0344800 0	0.666670 0	0.8619 1
Training Testing	Q	$\theta'(0)$	0.045310 0	0 .212860 0	0.045310 0	0.683570 0	1 1

Training Testing	R	0 	0 	0 	0 	0 	0 	0 	0 	0 0	1 1

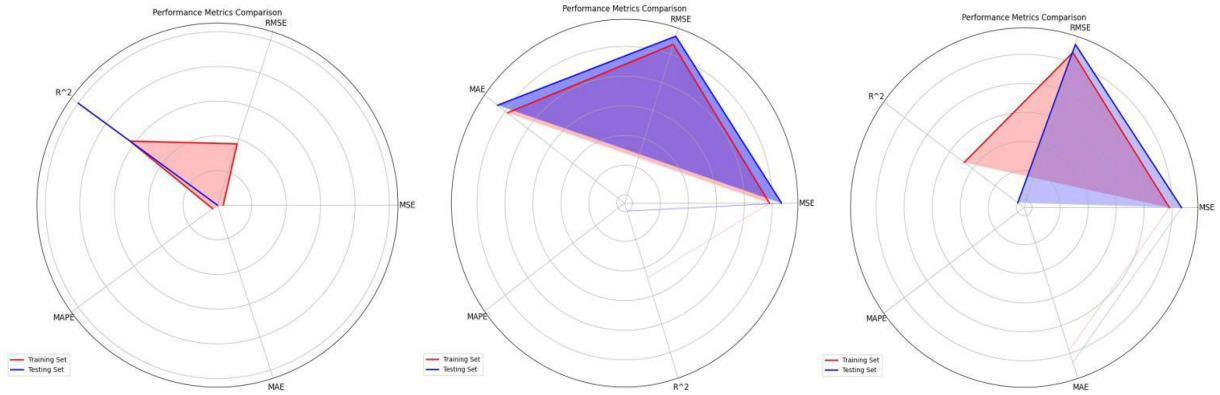

(a) **(b)** **(c)**

Fig. (7) Radar plot for evaluation metrics

5. CONCLUSIONS

The problems under consideration were addressed through numerical solutions, employing support vector machine simulations based on generalized principles for momentum and heat. Two-phase (Cu + SiO_2) and three-phase (Cu + Fe_3O_4 + SiO_2) nanoparticles suspended in water (H2O) were investigated for a comparative study.

- Increasing the magnetic parameter led to a reduction in the boundary layer thickness of momentum and thermal profiles. This finding holds significant promise for advancements in both industrial processes and scientific understanding.
- Nusselt number increases with mounting values of heat source parameter and similar trend is observed in the heat radiation parameter.
- Through numerical simulations of skin friction coefficient and Nusselt number, the support vector machine demonstrated its capability in accurately characterizing the physical phenomena of hybrid and ternary hybrid nanofluids with minimal error.
- Moreover, it was found that ternary hybrid nanofluids outperformed their dual-phase counterparts in terms of thermal performance over stretched sheets. This underscores the potential of employing tri-nanosized particle dispersions in base fluids for cooling applications.
- Radar plot displays evaluation metrics for training and testing datasets and increased values of MAE, RMSE and R^2 with respect to friction rate and nusselt number indicate a higher level of precision. This shows the effective ness of SVM in classifying the ternary hbrid nanofluids and hybrid nanofluids.

Acknowledgements: This research was supported by DST-CURIE-AI Centre (Phase-II)F2, Sri Padmavati Mahila Visvavidyalayam, Tirupati, A.P, India.

Nomenclature:

u, v velocity components in x, y direction

B_0induced magnetic field

$C_f$skin friction coefficient

$q_r$radiative heat flux

Q heat source/sink parameter

Nu Nusselt number

Pr Prandtl number

Cp specific heat at constant pressure

k^* mean absorption coefficient

M magnetic field parameter

T temperature of the fluid

Tw temperature of the wall

$T\infty$ ambient temperature

$U_w$velocity of stretching sheet

σ^* Stefan-Boltzmann constant

σ electrical conductivity of the fluid

ρdensity of fluid

ρC_pheat capacity

$\phi_1$volume fraction of copperparticles

$\phi_2$volume fraction of iron oxide particles

$\phi_3$volume fraction of silicon dioxide particles

f fluid

Nfnanofluid

hnfhybrid nanofluid

thnf ternary hybrid nanofluid

SVM Support vector machine

MSE Mean square error

MAE Mean absolute error

RMSE Root mean square error

REFERENCES

[1] ChoiS.U.S., Eastman J.A. Enhancing Thermal Conductivity of Fluids with Nanoparticles; Proceedings of the International Mechanical Engineering Congress and Exhibition; San Francisco, CA, USA. 12–17 November 1995.

[2] Chiam H.W., Azmi W.H., Usri N.A., Mamat R., Adam N.M. Thermal conductivity and viscosity of Al2O3 nanofluids for different based ratio of water and ethylene glycol mixture. *Exp. Therm. Fluid Sci.* 2017;81:420–429. doi: 10.1016/j.expthermflusci.2016.09.013.

[3] MKwizu MH, Makinde OD. Entropy generation in variable viscosity channel flow of nanofluids with convective cooling. C R Mechanique. 2015;343(1):38-56.

[4] Gbadeyan JA, Titiloye EO, Adeosun AT. Effect of variable thermal conductivity and viscosity on casson nanofluid floe with convective heating and velocity slip. Heliyon, 2020;6(1);3076.

[5] Xu H, Fan T, Pop I. Analysis of mixed convection flow of a nanofluid in a vertical channel with the Buongiorno mathematical model. Int Commun Heat Mass Transfer. 2013;44:15-22. doi:10.1016/j.icheatmasstransfer.2013.03.015.

[6] Haritha A, Vishali B, Venkata Lakshmi C. Heat and masstransfer of MHD Jeffrey nanofluid flow through a porous media past an inclined plate with chemical reaction, radiation, and Soret effects. Heat Transfer. 2022;1-20. doi:10.1002/htj.22735

[7] D. Huang,Z.Wu and B. Sunden, Effects of hybrid nanofluid mixture in plate heat exchangers, Exp.Therm.Fluid Sci. 72(2016), pp. 190-196.

[8] Emad.H Aly, Ioan Pop: MHD flow and heat transfer over a permeable stretching sheet in a hybrid nanofluid with convective boundary conditions; International journal of Numerical methods for heat and fluid flow, Vol.29 No.9,2019, pp.3012-3038, 0961-5539, DOI 10.1108/HFF-12-2018-0794.

[9] Venkateswarlu B, Satya Narayana p.V. Cu-Al_2O_3/H_2O hybrid nanofluid flow past a porous stretching sheet due to temperature-dependent viscosity and viscous dissipation. Heat transfer 2020;1-18. https://doi.org/10.1002/htj.21884.

[10] Malleswari Kakanti, Kata Sreelakshmi, Ganganapalli Sarojamma & Ali J. Chamkha (2022): Effect of stratification and non-linear radiant energy on MHD unsteady flow of Ag-Al_2O_3/$C_2H_6O_2$-water on an elongated surface, International Journal of Ambient Energy, DOI: 10.1080/01430750.2022.2029766.

[11] Khan,S.A,; Hayat, T;Alsaedi,A. Irreversability analysis for nanofluid flow (NiznFe2O4-C8H18 and MnZnFe2O4-C8H18) with radiation effect. Appl.Math.Comput. 2022,419,126879.

[12] Hayat T, Nadeem S. Heat transfer enhancement with Ag-Cuo/H2O hybrid nanofluid. Results Phys, 2017;7;2317-2324.

[13] Jafar Hasnain & Nomana Abid (2023) Numerical investigation for thermal growth in water and engine oil-based ternary nanofluid using three different shaped nanoparticles over a linear and nonlinear stretching sheet, Numerical Heat Transfer, Part A: Applications, 83:12, 1365-1376, DOI: 10.1080/10407782.2022.2104582.

[14] Manjunatha S.,Puneeth V.,Gireesha, B.J.,Chamkha, A.J. Theoretical Study of Convective Heat Transferin Ternary Nanofluid Flowing past a Stretching Sheet, J. Appl.Comput.Mech.,8(4),2022,1279–1286.https://doi.org/10.22055/JACM.2021.37698.3067

[15] Mousavi,S.M.; Esmaeilzadeh,F.; Wang,X.P. Effect of temperature and particles volume concentration on the thermophysical properties and the rheological behaviour of CuO/MgO/TiO_2 aqueous ternary hybrid nanofluid. J. Therm. Anal. Calorim. 2019,137, 879-901.

[16] W. Ashraf Adnan, Thermal efficiency in hybrid (Al2O3-CuO/H2O) and ternary hybrid nanofluids (Al2O3-CuO-Cu/H2O) by considering the novel effects of imposed magnetic field and convective heat condition, in: Waves in Random and Complex Media, 2022, https://doi.org/10.1080/17455030.2022.2092233.

[17] Kamel Guedri, Arshad Khan, Ndolane Sene, Zehba Raizah, Anwar Saeed, Ahmed M. Galal, "Thermal Flow for Radiative Ternary Hybrid Nanofluid over Nonlinear Stretching Sheet Subject to Darcy–Forchheimer Phenomenon", Mathematical Problems in Engineering, vol. 2022, Article ID 3429439, 14 pages, 2022. https://doi.org/10.1155/2022/3429439.

[18] Vishalakshi,A.B.; Mahabaleshwar,U.S.;Laroze,D.;Zeidan,D. “Astudy of mixed convective ternary hybrid nanofluid flow over a stretching sheet with radiation and transpiration”, Special topics and reviews in Porous media ,2023, doi: 10.1615/SpecialTopicsRevPorousMedia.2023046513.

[19] Sharma, R.P., Badak, K. Heat transport of radiative ternary hybrid nanofluid over a convective stretching sheet with induced magnetic field and heat source/sink. *J Therm Anal Calorim* (2024). https://doi.org/10.1007/s10973-024-12979-y .

[20] Ramesh GK, Madhukesh JK, Shehzad SA, Rauf A. Ternary nanofluid with heat source/sink and porous medium effects in stretchable convergent/divergent channel. *Proceedings of the Institution of Mechanical Engineers, Part E: Journal of Process Mechanical Engineering*. 2024;238(1):134-143. doi:10.1177/09544089221081344

[21] Brenner M.P., Eldredge J.D., Freund J.B.Perspective on machine learning for advancing fluid mechanics.Phys. Rev. Fluids, 4 (2019), Article 100501

[22] Rehman, K.U.; Shatanawi, W. Non-Newtonian Mixed Convection Magnetized Flow with Heat Generation and Viscous Dissipation Effects: A Prediction Application of Artificial Intelligence. *Processes* **2023**, *11*, 986. https://doi.org/10.3390/pr11040986.

[23] Priyadharshini P., Vanitha Archana M., Ameer Ahammad N., Raju C.S.K., Yook Se-jin, Shah Nehad Ali, Gradient descent machine learning regression for MHD flow: Metallurgy process .Int. Commun. Heat Mass Transfer, 138 (2022), Article 106307

[24] Baazeem, A.S.;Arif,M.S.;Abodayeh,K. An Efficient and Accurate Approach to Electrical Boundary layer Nanofluid Flow Simulation: A use of Artificial Intelligence. *Processes* **2023**, *11*, 2736.https://doi.org/10.3390/pr11092736.

[25] Priyadarshini,P.;Archana,M.V.;Shah,N.A.;Alshehri,M.H. Ternary hybrid nanofluid flow emerging on a symmetrically stretching sheet optimization with Machine Learning Prediction Scheme. *Symmetry* **2023**, *15*, 1225.https://doi.org/10.3390/sym15061225.

[26] Oyehan, T.A.; Liadi, M.A.; Alade, I.O. Modeling the efficiency of TiO2 photocatalytic degradation of MTBE in contaminated water: A support vector regression approach. SN Appl. Sci. **2019**, 1, 386. [CrossRef].

[27] Haritha, A.;Sarojamma, G.; Radiation effect on heat and mass transfer in MHD flow of a casson fluid over a stretching sheet. Int. J. of sci. and innovative research. 2014;2(6);2347-3142.

[28] Saeed,U.J; Umar Khan; Magda,A.E.R.; Saeed, I.;Hassan,A.M.;Aman,U., Effect of variable thermal conductivity of ternary hybrid nanofluid over a stretching sheet with convective boundary conditions and magnetic field. Results in Engineering, (20)2023, 101531. https://doi.org/10.1016/j.rineng.2023.101531.

[29] Lu, C.J.; Lee, T.S.; Chiu, C.C. Financial time series forecasting using independent component analysis and support vector regression. *Decis. Support Syst.* 2009, *47*, 115–125.

[30] Mamatha, S.U.; Devi, R.L.V.R.; Ahammad, N.A.; Shah, N.A.; Rao, B.M.; Raju, C.S.K.; Khan, M.I.; Guedri, K. Multi-linear regression of triple diffusive convectively heated boundary layer flow with suction and injection: Lie group transformations. *Int. J. Mod.Phys. B* 2022, *37*, 2350007.

[31] Shah Jahan; Hamzah, S; Nazar, R; Ioan Pop. Analysis of heat transfer in nanofluid past a convectively heated permeablestretching/shrinking sheet with regression and stability analyses. *Results in physics* 10(2018)395-405.

[32] Khan, W.A.; Pop, I. Boundary layer flow of a nanofluid past a stretching sheet. *Int. J. Heat Mass Transfer.* **2010**, *53*, 2477–2483.